

ACTIVE SUSPENSION SYSTEM IN PARALLEL HYBRID ELECTRIC VEHICLES

Morteza Montazeri-Gh & Mahdi Soleymani

Abstract: *In previous studies, active suspension system in conventional powertrain systems was investigated. This paper presents the application of active suspension system in parallel hybrid electric vehicles as a novel idea. The main motivation for this study is investigation of the potential advantages of this application over the conventional one. For this purpose, a simultaneous simulation is developed that integrates the powertrain and active suspension systems in a unified media where the power and input data between two systems are exchanged. Using this concurrent simulation tool, the impact of the active suspension load on the internal combustion engine response is studied for both conventional and hybrid electric configurations. The simulation results presented in this study show that there are quite remarkable advantages for application of the active suspension in parallel hybrid electric vehicles in comparison with the conventional one.*

Keywords: *Active Suspension System, Hybrid Electric Vehicle, Simultaneous Simulation*

1. Introduction

The purpose of an automobile suspension is to adequately support the chassis, to maintain tire contact with the ground, and to manage the compromise between vehicle road handling and passenger comfort [1]. Suspension systems can be classified as passive, semi-active, and active suspension (AS) systems. In order to positively influence these properties, active components are introduced. Active components enable the suspension system to adapt to various driving conditions. By adding a feedback controlled actuator, the vehicle driving comfort and safety can be considerably improved compared to a suspension setup with fixed properties [2].

Application of AS in conventional vehicles has been investigated extensively in previous studies. Previous studies have reported that the application of AS system in conventional vehicles encounters some obstacles [3]. One of the drawbacks in conventional vehicles is that the power required for the AS system is directly supplied by the vehicle internal combustion engine (ICE). In this case, the ICE requires time to adjust itself to the time-varying AS loads due to its dynamics. If the AS loads vary faster than the engine can adjust, then, the suspension will not function properly temporarily. Consequently, the vehicle may hesitate. If, on the other

hand, the load gets reduced too fast, the vehicle surge may occur [3]. As a result, the ICE dynamics is a major concern for the AS system in conventional vehicles. Moreover, AS loads may shift the ICE operating points to the inefficient regions where the instant emissions and fuel consumption may be increased.

Hybrid electric vehicle (HEV) is one of the most viable solutions to the world's need for cleaner and more fuel-efficient vehicles. In order to overcome the drawbacks of conventional vehicles, HEVs encompass two energy converters to generate the power required to drive the vehicle. Most typically, the architecture of HEV includes an ICE with an associated fuel tank and an electric machine with its associated energy storage system (ESS) i.e. battery. The powertrain system for a parallel hybrid electric vehicle incorporates two power drives including an ICE and an electric motor (EM). In HEVs, unlike the conventional vehicles, the vehicle subsystems may be powered by either mechanical ICE or the electrical power sources. This can be especially helpful when one of the power sources can not provide the required power due to its performance constraints. Moreover, HEVs can provide the capability of regeneration of the AS energy while it is working in a power recovery mode [4 and 5].

In this paper, the idea of the application of AS system in HEVs is presented. The main motivation for this study is investigation of the potential advantages for this application over the conventional one. For this purpose, and as a preliminary goal, a simulation tool is developed in which the suspension and powertrain systems are simulated simultaneously. In this approach, the powertrain and AS systems simulations are

Paper first received March. 05, 2008. and in revised form Sep. 15. 2009.

Morteza Montazeri-Gh is Associate Professor with the Department of Mechanical Engineering and director of Systems Simulation and Control Laboratory at Iran University of Science and Technology, Tehran. montazeri@iust.ac.ir

Mahdi Soleymani is a PhD student at the same Department. m_soleimani@iust.ac.ir

integrated in order to study the exchange of power and data between AS and powertrain systems. Using this concurrent simulation approach, the idea of AS application in HEV is studied from energy and performance points of view.

The structure of the paper is as follows. The simulation and control of AS system is firstly described. The powertrain system simulation for both conventional and hybrid electric vehicles are then presented. In addition, the fuzzy-based control approach employed for HEV power management is described. Finally, the simultaneous simulation approach is introduced and the simulation results and analysis are discussed.

2. Active Suspension Simulation and Control

AS simulation and control is presented in this section. The vehicle suspension dynamic equations of motion are firstly presented. The influence of the speed pattern on the time-domain disturbances of the suspension system is then discussed. Finally, the control method used for active suspension is described.

2-1 Suspension System Dynamic Equations of Motion

In this study, a full-vehicle model (Fig. 1) is used for the suspension system simulation. This model is a suitable choice for the ride quality evaluation as it captures the effective motions for the ride comfort assessment i.e. body bounce, pitch and roll accelerations.

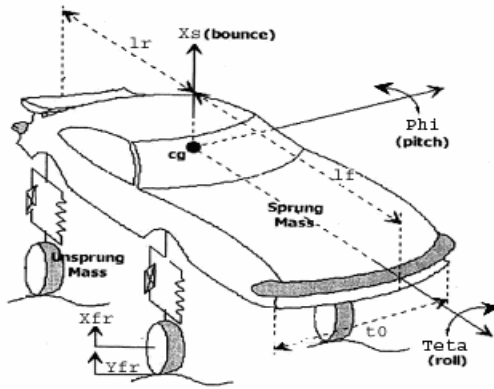


Fig. 1. Suspension system in a 7 DOF vehicle model.

The governing dynamic equations of motion for this model in a matrix form are as follows:

$$M \ddot{X} + C \dot{X} + K X = F U \quad (1)$$

$$X = \{x_s; \phi; \theta; \dot{x}_s; \dot{\phi}; \dot{\theta}; x_{ufr}; x_{ufr}; x_{urr}; x_{urr}\}$$

Where, M , K , C , and F are mass, stiffness, damping, and forcing matrices respectively. X denotes the state vector whose elements are body bounce, pitch, and roll motions and their derivative as well as unsprung masses vertical displacement and their derivative respectively. It is assumed that body and wheel displacements are measured from their static

equilibrium position. Tire-road holding force is also modeled as a nonlinear function as follows:

$$F_{holding} = K_t (x_u - x_0) \quad \text{if } (x_u - x_0) \leq \Delta_{stat}$$

$$F_{holding} = 0 \quad \text{if } (x_u - x_0) \geq \Delta_{stat} \quad (2)$$

where, K_t , x_u , x_0 , and Δ_{static} are tire stiffness coefficient, unsprung mass displacement, road displacement disturbance, and suspension spring static deflection, respectively.

2-2. Environmental Inputs

Road time-domain disturbance depends not only on the road profile geometry, but also the vehicle speed. Therefore it is essential to consider the effect of the driving pattern on the time-domain disturbance of the suspension system. The concept of the influence of the speed pattern on the suspension system disturbance can be described when a vehicle is moving on a sine wave road with a variable speed driving pattern. Since the frequency content of the transmitted vibrations to the vehicle depends on the vehicle speed, the passengers' perception of the transmitted vibrations varies with the speed variations. In the real traffic condition, the vehicle speed varies frequently and these speed fluctuations should be considered in the time-domain ride evaluation of the suspension system [6].

2-3. AS System Control Design

For control purpose of the AS system, the fully active skyhook control approach [7] is employed. In this method, the well-known 'skyhook' control strategy patented by Karnop [8] is employed for the control force calculation. As the name implies, the skyhook configuration has a damper connected to some inertial reference in the sky, as shown in Fig. 2.

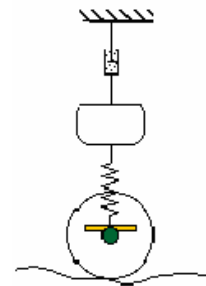


Fig. 2. Skyhook model.

In order to implement the skyhook control law to the full-vehicle model, it is assumed that the body is suspended at its corners by the skyhook dampers. Considering this scenario, the full-vehicle model has been divided to four separate quarter models. The logic behind this control design is that, reducing transmitted forces from suspension system to the body at its corners, the total transmitted forces to the body are reduced. This reduction, consequently, will result in

reduction of the body bounce, pitch and roll accelerations. In other words, the vehicle body motion is controlled by the AS actuators forces at four corners of the body. These forces are calculated at each corner using the skyhook control strategy.

Fully active control states that the required control force is equal to the product of the sprung mass velocity and the skyhook damping coefficient as equation 4 implies, and therefore is capable of putting energy into the system as well as take energy out. This makes fully active control a powerful tool in affecting the motion of the sprung mass [7].

The AS system equations of motion are as equation 3.

$$\ddot{x}_s = -\frac{1}{m_s} \left[k_s(x_s - x_u) + c(\dot{x}_s - \dot{x}_u) + F \right] \quad (3)$$

$$\ddot{x}_u = -\frac{1}{m_u} \left[-k_s(x_s - x_u) - c_s(\dot{x}_s - \dot{x}_u) + k_t(x_u - x_0) - F \right] \quad (4)$$

$$F_{act} = -C_{skyhook} \cdot \dot{x}_s$$

Where $C_{skyhook}$ is the skyhook coefficient. In the AS model, the stiffness coefficients of the suspension springs are lowered up to three fourths of their original values. AS instant power consumption demanded continuously from the powertrain system is calculated using equation 5.

$$P_{act} = F_{act} \cdot V_{act} = -C_{skyhook} \cdot \dot{x}_s \cdot (\dot{x}_s - \dot{x}_u) \quad (5)$$

3. Powertrain Simulation

In this section, the powertrain simulation is described. The main objective of the powertrain simulation is obtaining an acceptable estimation of the fuel consumption (FC) and exhaust emissions of conventional vehicle and HEV in the presence of AS load. This objective is reflected in the simulation approach. The powertrain simulation method used in this study incorporates a backward-facing approach [9]. Backward-facing approach is shown in Fig. 3 as a schematic diagram.

This approach does not require any model for driver behavior. Instead, a driving cycle is tracked by the vehicle. The driving cycle is a velocity versus time speed profile which represents the driving pattern in a specific geographical region.

Vehicle required traction force and velocity are then translated into the required torque and velocity that must be provided by the vehicle wheel and other components upstream. This calculation approach carries backward through the driveline against the tractive power flow direction until the fuel use and/or the electrical energy use that would be necessary to meet the trace is computed. Backward approach

depends on the ICE characteristic maps to a great extent.

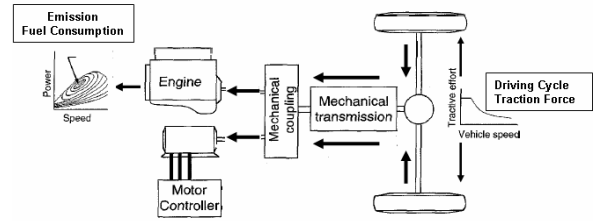


Fig. 3. Backward facing simulation approach schematic diagram

The ADvanced VEHICLE Simulator (ADVISOR) [9] and MATLAB-SIMULINK are used for simulation study. ADVISOR employs a combined forward/backward facing approach for the vehicle performance simulation. Simulations are performed for both conventional and HEVs. In the former case, AS required power is demanded directly from the combustion engine while in the later one it is demanded from HEV power bus. The simulation parameters as well as the vehicle components models have been set for a parallel HEV and a conventional vehicle designed in the previous studies [10].

4. Hybrid Electric Powertrain Control

Fuzzy control approach is employed to devise HEV control design in this study. The main objective of the fuzzy controller is to cause the ICE to work in the vicinity of its optimal operating points [11].

The optimal operating points of the engine are determined based on ICE parameters at the current vehicle speed to minimize instantaneous FC and emissions. At any particular point in time, the speed of rotation for the ICE is determined based on the powertrain configuration and the current gear ratio. This is the speed at which the instantaneous optimisation is performed. For the current speed, all possible torques that the ICE can provide are considered. Then the FC and emissions (HC, CO and NOx) for all torques at the current speed are taken from the engine maps and the following cost function is calculated for all of these points:

$$j = \frac{1}{w_1 + w_2 + w_3} \left(w_1 \frac{FC}{FC} + w_2 \frac{HC + NO_x}{HC + NO_x} + w_3 \frac{CO}{CO} \right) \quad (6)$$

in which all variables are normalized to their corresponding target value limits. The target value of the FC is defined by the designer while for the emissions, the standards of tailpipe emissions are used. Moreover, w_i 's are relative weights which are assigned to each parameter based on their importance. This is one large degree of freedom, and the weights must be selected based on the design objectives. For instance, when the main objective is the minimization of the vehicle FC, the weight of FC is set to 1 and the weights

of emissions will be set to zero. In this study, PNGV passenger car constraints [12] are used to ensure that the vehicle performance is not sacrificed during the trade off solution.

The actual torque delivered by the ICE must be determined such that the driver's torque requests (from brake and accelerating pedals) are satisfied consistently and the battery is sufficiently charged at all times. Therefore, the actual output torque of the ICE is computed by fuzzy control strategy based on the optimal operating point of the ICE, driver's torque request and the battery state of charge (SOC). The remaining torque at that speed, required to meet driver's command is provided by the EM. The EM may produce either positive or negative torque. A schematic of this control strategy is shown in Fig. 4. The FLC design details have been described in a previous work [10].

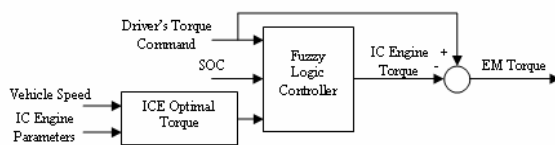


Fig. 4. Hybrid Powertrain Control Strategy.

5. Simultaneous Simulation of Powertrain and AS Systems

In order to study the AS and powertrain systems simulations in a unified media, a simultaneous simulation tool is developed in this study. The simultaneous simulation concept is introduced in this section.

The problem of simultaneous simulation is studied from three aspects including environmental input, vehicle dynamics, and energy interaction.

The environmental inputs of the suspension and powertrain systems are quite different. Suspension system main disturbances include the road irregularities modelled by either random or bumpy signals, while the powertrain system input relates to the vehicle speed pattern represented by a predefined driving pattern. In addition, suspension system input depends strongly on vehicle speed which is determined by the driving pattern. Therefore, the suspension system disturbance must be tuned continuously according to vehicle speed.

Different dynamics of the systems is the other concern. Powertrain simulation is mainly based on the quasi-steady simulation approach in which steady-state characteristic maps of the components are employed for calculations. However, suspension system dynamics is introduced by much faster differential equations. In this case, due to the quasi-steady assumption, the required numerical discrete time-step for the powertrain is far greater than the AS system one. The acceptable numerical time-step is therefore crucial in the simultaneous simulation of these two systems.

Finally, AS and powertrain systems have an interaction in terms of energy. The AS required power is demanded from the powertrain system continuously. The energy interactions of AS and powertrain systems in conventional vehicle and HEV are also different. In the conventional vehicles, this power load is imposed on the combustion engine while, in the HEVs it may be demanded from the ESS.

In this study, energy interaction of conventional and HEVs has been considered separately. In the conventional vehicle, the AS load is modelled as an extra torque added up to the engine required torque as shown in Fig. 5. In the HEV, however, this load is considered as an additional electrical accessory load requested from the electrical power bus as shown in Fig. 6. The total required electrical power bus is then provided by the generator or ESS, according to the control strategy.

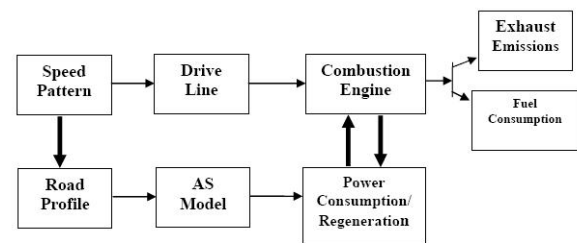


Fig. 5. Data flow for simultaneous simulation of AS and conventional powertrain systems

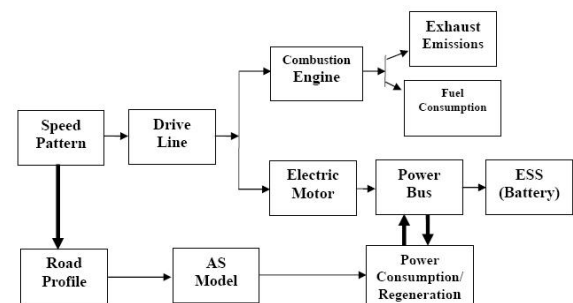


Fig. 6. Data flow for simultaneous simulation of AS and HEV powertrain systems

6. Simulation Study and Results Analysis

Computer simulation results are presented in this section. The simulations are performed for the mentioned powertrain-suspension combinations. The suspension parameters are set as table 1.

Moreover, the hybrid electric powertrain parameters are set for a parallel HEV with the following specifications:

_ Gearbox: five speed manual gearbox with following gear ratios; 2.84, 3.77, 5.01, 5.57 and 13.45. It should be noted that final drive ratio has been included in gearbox ratio.

Efficiency of gearbox is assumed 95%.

- _ IC engine: 41kW SI engine, obtained by scaling of Geo Metro 1.0 l SI engine.
- _ Electric motor: 13.5kW AC motor, obtained by scaling of Westinghouse AC induction motor with a maximum power output of 75 kW.
- _ Energy storage system: 14 12V Hawker Genesis valve-regulated lead-acid battery, model 12V26Ah10EP.
- _ Catalyst converter: close-coupled conventional converter for an SI engine.

Tab. 1. 7 dof model parameters values.

| Description | Symbol | Value |
|--|-----------------|----------------------------------|
| Sprung mass | m_s | 1375.9 kg |
| Sprung mass moment of inertia about x-/y- axis | I_x/I_y | 484.4 / 2344.4 kg.m ² |
| Unsprung mass (front/rear) | m_f/m_r | 40 / 40 kg |
| Vehicle stiffness of tire (front/rear) | k_{tf}/k_{tr} | 182087 / 182087 N/m |
| Suspension stiffness (front/rear) | k_{sf}/k_{sr} | 20984.8 / 19121.7 N/m |
| Suspension damping coefficient (front/rear) | c_{sf}/c_{sr} | 2400 / 2500 N.s/m |
| Track | t_0 | 0.144 m |
| Wheel base | L | 2.63 m |
| Distance between y-axis and (front/rear) tires | l_f/l_r | 1.12 / 1.51 m |

The size of the engine and electric motor and the number of battery modules are obtained based on a previous study through a scaling technique using a GA approach [10]. Besides, for the conventional powertrain simulation, the scaled version of the HEV combustion engine is used. Furthermore, the powertrain system time-step has been fined up to an acceptable AS time-step level. This will not violate the simulation results of the powertrain system in the backward-facing approach. Instead the run time will increase considerably.

Combining the road disturbances and the driving patterns, two combined disturbances are developed for the suspension system as listed in table 2.

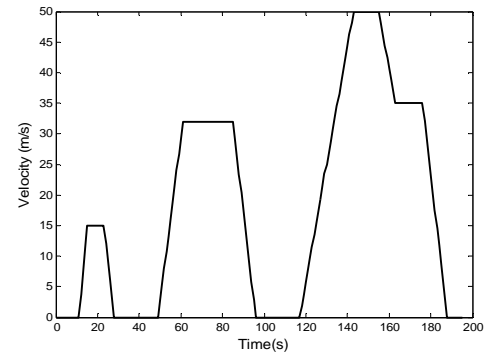
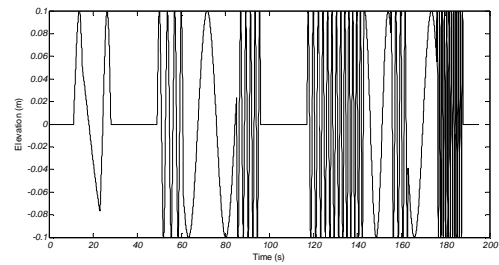
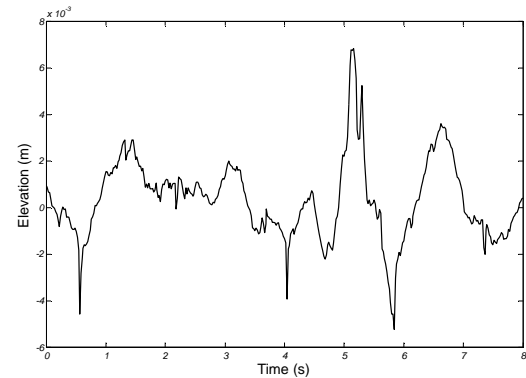
Tab. 2. Combined road-driving pattern disturbance setups.

| Combined Disturbance | Road | Speed Pattern | Suspension Disturbance |
|----------------------|--------|----------------|------------------------|
| I | Bumpy | ECE | Bumpy-ECE |
| II | Random | Constant Speed | Random-Constant |

In the first setup, the vehicle traces the ECE speed pattern (Fig. 7) while it passes over a bumpy road. In the second setup, it is assumed the vehicle is running over the random road with constant 80 km/hr velocity. Fig. 8 depicts the combined Bumpy-ECE disturbance.

Fig. 9 also shows the time-domain random road disturbance at the constant velocity.

In the simulations with the combined Bumpy-ECE disturbance, the engine is started at the cold condition while in the simulations with the Random-Constant disturbance; it is started at hot condition.

**Fig. 7. ECE driving pattern****Fig. 8. Combined ECE-Bumpy disturbance****Fig. 9. Random road disturbance**

Figures 10 and 11, respectively, illustrate the vehicle body bounce and pitch accelerations with active and passive suspension systems in the presence of the combined Bumpy-ECE disturbance. As it is seen in these figures, AS system has caused considerable decrease in the transmitted accelerations to the body. Moreover, the speed variations apparently affect the transmitted vibrations to the body implying the influence of the speed pattern on the ride comfort. In this case, the amplitudes and frequencies of the transmitted accelerations increase with speed increase.

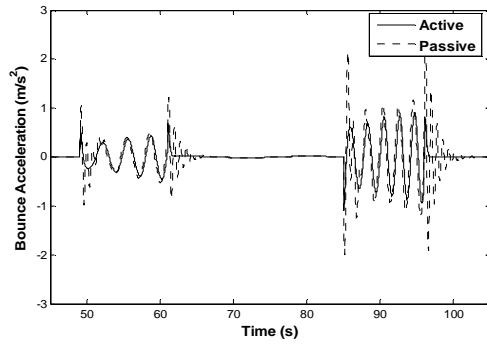


Fig. 10. Body bounce acceleration for Bumpy-ECE combined disturbance

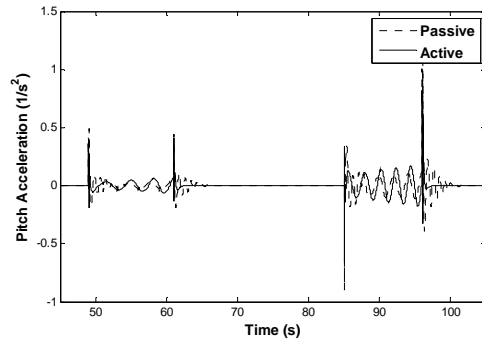


Fig. 11. Pitch acceleration for Bumpy-ECE combined disturbance

Figures 12, 13 illustrate the power consumption for the combined Random-Constant and Bumpy-ECE disturbances respectively. As it is seen in Fig. 13, the AS instant power demand increases dramatically with vehicle velocity increase for the Bumpy-ECE combined disturbance.

It can be stated at this point that the vehicle speed pattern affects both vehicle ride quality and AS system energy consumption. This is an important conclusion that implies the use of an adaptive control system when a vehicle is experiencing different road profiles and driving conditions.

Table 3 shows the vehicle emissions and FC results. As it can be seen in this table, AS system load has caused an increase in the FC and emissions of both conventional vehicle and HEV. However this increase is more considerable for the Bumpy-ECE road-cycle disturbance, where AS system instant power demand is much more than the one for Random-Constant road-cycle disturbance (Figures 12 and 13).

Moreover, since combustion chamber temperature has a pronounced effect on the emissions [13], the emissions are apparently reduced for the Random-Constant case that the ICE is started at the hot condition. Figures 14 and 15 show the combustion engine operating points for conventional and hybrid electric powertrain systems, respectively, using the combined Bumpy-ECE disturbance. As it is seen in these figures, the AS load causes an upward shift in the combustion engine required torque.

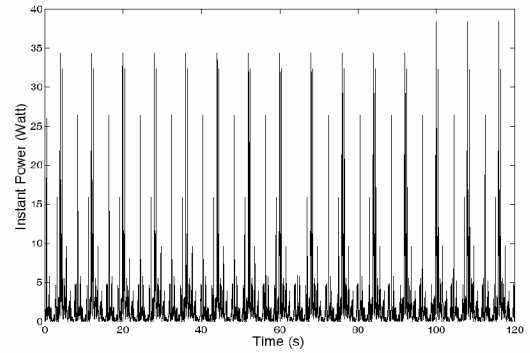


Fig. 12. Instant power consumption of AS for Random-Constant road-cycle disturbance.

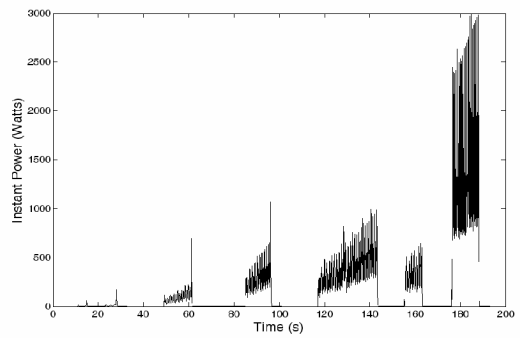


Fig. 13. Instant power consumption of AS for Bumpy-ECE road-cycle disturbance.

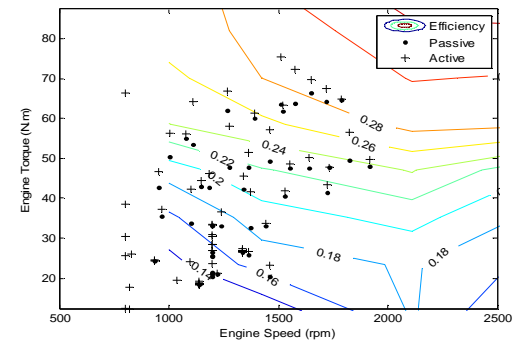


Fig. 14. ICE operating points for conventional vehicle with combined Bumpy-ECE disturbance.

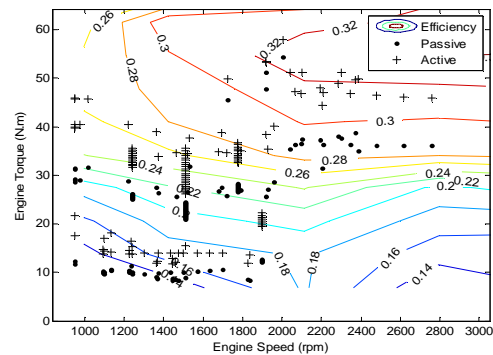
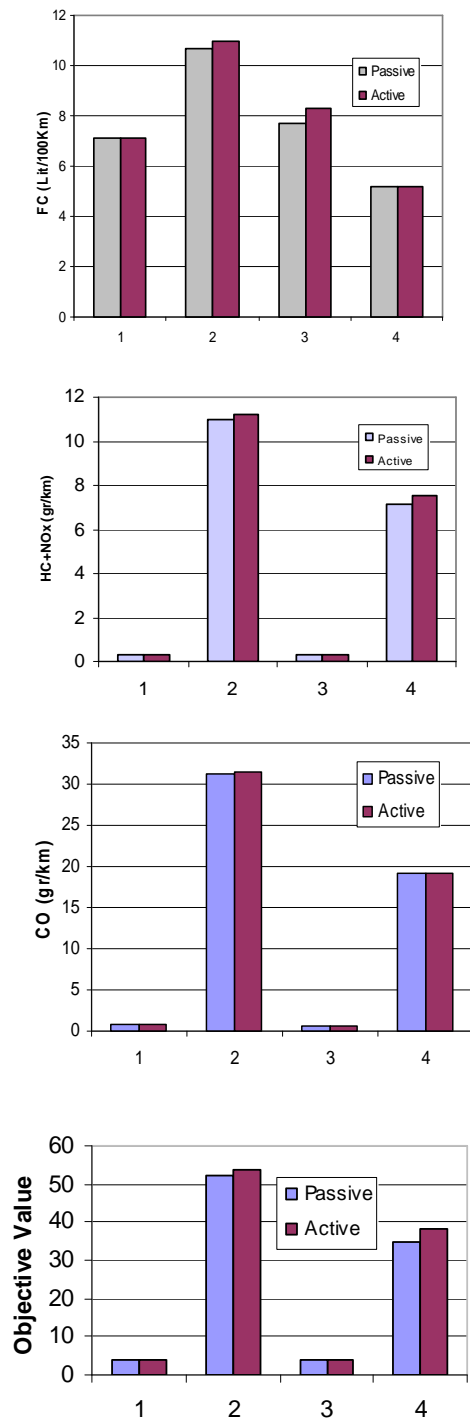


Fig. 15. ICE operating points for HEV with combined Bumpy-ECE disturbance

Tab. 3. Emissions and fuel consumption results



- 1: conventional, Random-Constant
 2: conventional, Bumpy-ECE
 3: HEV, Random-Constant
 4: HEV, Bumpy-ECE

In order to further study the effect of AS load on the powertrain system, the engine required torque is examined more precisely. Figures 16 and 17 depict the combustion engine required torque for the conventional vehicle and HEV powertrain systems respectively.

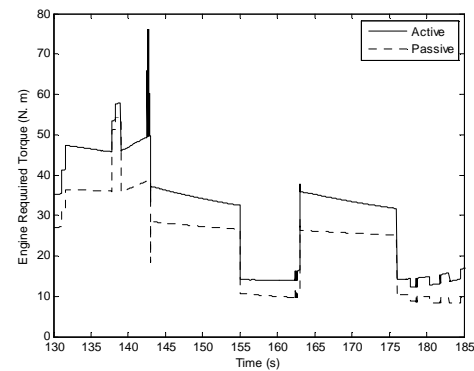


Fig. 16. ICE required torque for HEV with the combined Bumpy-ECE disturbance

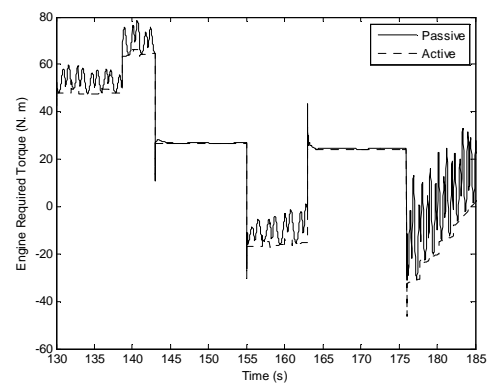


Fig. 17. ICE required torque for the conventional vehicle with combined Bumpy-ECE disturbance

In the conventional powertrain system, the ICE is affected apparently by the AS load dynamics as shown in Fig. 17. As it is seen in this figure, the AS load is translated as a high frequency torque load applied to the ICE. However, as the combustion engine requires time to adjust to the time-varying loads imposed on it, it is not capable of providing the AS system with the required power, and therefore, a power shortage is occurred. On contrary, the AS load in hybrid electric powertrain system causes a relatively uniform shift in the engine required torque signal as shown in Fig. 16. In HEV, a share of the AS power demand is provided by the electrical ESS. Figures 18 and 19 depict the SOC history without and with AS load, respectively. The SOC history without the AS load is a smooth diagram as shown in Fig. 18. However, as it is seen in Fig. 19, some ripples are seen in the SOC history of the ESS while it is experiencing the AS load.

7. Conclusion

The idea of application of AS system in HEV is studied in this paper. A simultaneous simulation approach in which AS and powertrain systems are simulated concurrently is proposed for this purpose. In the simulation approach, data and energy interactions are modeled.

Simulation results reveal that the AS load causes an

increase in FC and emissions of both conventional vehicle and HEV. However, in the conventional vehicle, the AS load is translated as an additional high-frequency torque load on the combustion engine while in the HEV, it causes a smooth upward shift in the combustion engine torque. Therefore, in conventional vehicle, due to slow response dynamics of combustion engine, the AS power shortage as well engine hesitation and surge are more likely to occur. In addition, the simulation results prove the effectiveness of the idea of AS system application in the HEV as an alternative platform for AS system power supply.

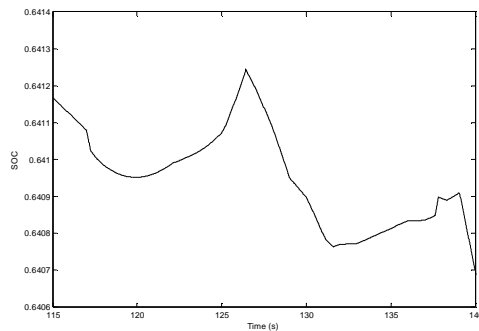


Fig. 18. SOC for HEV with Bumpy-ECE disturbance and passive suspension system

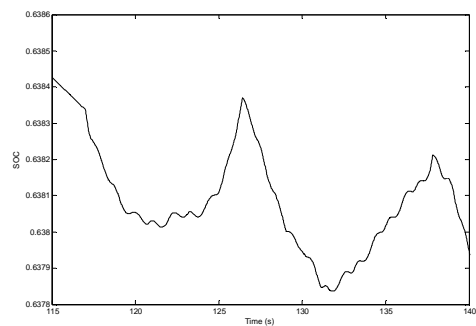


Fig. 19. SOC for HEV with Bumpy-ECE disturbance and active suspension system

References

- [1] Hac, A., "Optimal Linear Preview Control of Active Suspension", *Vehicle System Dynamics*, Vol. 21, 1992, pp. 167-195.
- [2] Fischer, D., Isermann, R., "Mechatronic Semi-Active and Active Vehicle Suspensions", *Control Engineering Practice*, 12, 2004, pp. 1353-1367.
- [3] Mrad, R.B., Fassois, S.D., Levitt, L.A., "A Polynimial-Algebraic Method for Non-Stationary TARMA Signals Analysis- Part II: Application to Modeling and Predicting Power Consumption in Automobile Active Suspension Systems", *Signal Processing*, 65, 1998, pp. 21-38.
- [4] Montazeri-Gh, Kashani, M., "Energy Regeneration of Active Suspension System in Hybrid Electric Vehicles", *Advanced Vehicle Control Conference*, Japan, 2002.
- [5] Ping. Hsu, "Power Recovery Property of Electrical Active Suspension Systems" *IEEE*, 96024, 1996.
- [6] Montazeri-Gh, M., Jazayeri-M, S.Y., Soleymani, M., 'Vehicle Ride Evaluation Based on a Time-Domain Variable Speed Driving Pattern', *International Journal of Vehicle Design*, Vol. 47, Nos. 1/2/3/4, pp.81-101, 2008.
- [7] Goncalves, F.D., "Dynamic Analysis of Semi-Active Control Techniques for Vehicle Applications", M.S.C Dissertation, Virginia Polytechnic Institute and State University, 2001.
- [8] Karnopp, D., Crosby, M.J., "System for Controlling the Transmission of Energy Between Spaced Members". United States Patent #3,807,678, 1974.
- [9] Wipke, K.B., Cuddy, M.R., Burch, S.D., "ADVISOR 2.1: a User-Friendly Advanced Powertrain Simulation Using a Combined Backward/Forward Approach", *IEEE Trans. Vehicular Technology*, 48 (6), 1999, pp. 1751-1761
- [10] Montazeri, M., Poursamad, A., B. Ghalichi, "Application of Genetic Algorithm for Optimization of Control Strategy in Parallel Hybrid Electric Vehicles", *Journal of the Franklin Institute*, 343, 2006, pp. 420-435.
- [11] Johnson, V.H., Wipke, K.B., Rausen, D.J., "HEV Control Strategy for Real-Time Optimization of Fuel Economy and Emissions". *Proceedings of the Future Car Congress*, SAE Paper No. 2000-01-1543, 2000.
- [12] Moore, T.C., Lovins, A.B., "Vehicle Design Strategies to Meet and Exceed PNGV Goals", *Electric and Hybrid Vehicles—Implementation of Technology SAE Special Publication SP-1105*, 1995, pp. 79-121.
- [13] Schafer, F., Basshuysen, R.V., *Reduced Emissions and Fuel Consumption in Automotive Engines*, 1995.